NASA TT F-9871

EXPERIMENTAL AND THEORETICAL RESULTS ON HEAT TRANSFER AT THE LEADING EDGE OF HYPERSONIC SWEPTBACK WINGS

J.Valensi, R.Michel, and D.Guffroy

Translation of "Résultats expérimentaux et théoretiques sur le transfert de chaleur au bord d'attaque des ailes à forte flèche en hypersonique".
AGARD, Recent Developments in Boundary Layer Research, Part 2, pp.889-907, May 1965.

NATIONAL AERONAUTICS AND SPACE ADMINISTRATION
WASHINGTON JANUARY 1966

EXPERIMENTAL AND THEORETICAL RESULTS ON HEAT TRANSFER AT THE LEADING EDGE OF HYPERSONIC SWEPTBACK WINGS

J.Valensi, R.Michel, and D.Guffroy

This paper is devoted to a survey of the theoretical and experimental results on laminar heat transfer at the leading edge of hypersonic wings. The results of pressure and transfer heat rate measurements at the stagnation line of leading edges at Mach numbers 4, 7, and 10 are presented. Two techniques of theoretical analysis are described and illustrated; they are based on the solution of the local and global boundary layer equations respectively. The theoretical and experimental results are in satisfactory agreement in the case of large sweep angle but the effect of a strong entropy gradient due to the curvature of the shock wave is evident in the case of medium sweep at high speed.

Author

1. Introduction

The study of heat transfer in the region of the stagnation point of space vehicles is quite advanced, at least for the case of a laminar boundary layer; however, a second less known critical region, present in a hypersonic glider, is the leading edge of the wing of which such a glider consists, in which case the prediction of heat transfer to the wall necessitates an analysis of the development of the boundary layer in a three-dimensional flow.

Presently available theoretical results concern mainly the case of an in-

* Numbers in the margin indicate pagination in the original foreign text.

finite sweptback cylinder. For this type of body, similitude solutions, as derived specifically by Reshotko and Beckwith (Bibl.1), yield simple formulas for the heat transfer along the stagnation line of the leading edge.

However, the use of formulas of the infinite cylinder, in estimating the heat flux at the leading edge of a real wing, is disputable already at short distances from the nose since the so-called origin effect might considerably modify the results. In addition, these formulas yield no data on the evolution of the heat transfer at the point of attachment of wing tip to leading edge, where both pressure and Mach number may undergo variations which, to a nonnegligible extent, will influence the development of the boundary layer and its principal characteristics.

To find some answer to these various questions, a study on the theoretical and experimental aspects of the problem has been started jointly by the Institute of Fluid Mechanics of Marseille and the National Aerospace Research and Development Administration. The present paper resumes and completes a partial analysis published previously (Bibl.2) and gives theoretical and experimental considerations discussed in two papers published in the Comptes Rendus of the Academy of Sciences (Bibl.3, 6).

In the experimental sector, the program included measuring the pressure distributions and the heat transfer to the wall along the leading edge of two hypersonic wing models. The overall results are reported for different angles of sweepback of the leading edge, at Mach numbers of 4, 7, and 10.

In the theoretical field, two different calculation methods were de- /890
fined and utilized. One is based on the solution of local equations of the boundary layer and on solutions of local similitude; the other method uses a solution of the summary equation of energy. Both methods make use of the prin-

ciple of superposition in the boundary layer of the longitudinal flow on the transverse flow.

2. Experimental Study

2.1 Test Conditions

The experimental study covered three wing models, representing a schematic hypersonic glider provided with a spherical-sector tip, attached to a leading edge of the same radius with two plane faces. The experimental program scheduled pressure measurements and determinations of the heat transfer to the wall along the stagnation line. The models were placed at zero incidence, while the angle of sweepback of the leading edge was varied with the sideslip.

2.1.1 Tests at Mach Numbers 4 and 7

The model A had the following geometric characteristics: sweepback, 80°; radius of tip and leading edge, 7 mm ($M_{\infty} = 4$) or 10 mm ($M_{\infty} = 7$); overall length, 160 mm ($M_{\infty} = 4$) or 265 mm ($M_{\infty} = 7$).

At Mach 4, the tests were made in the supersonic wind tunnel of the IMFM (Institute of Fluid Mechanics, Marseille). In this case, the base temperature is close to the wall temperature ($\sim 290^{\circ}K$). The test Mach number was $M_{\infty} = 3.95$. The base temperature was regulated by means of a reheater, so as to obtain deviations of a few degrees relative to the temperature of the mockup (ambient temperature).

The measuring principle for the heat transfer consisted in recording, as a function of time, the rise in temperature of red copper pellets of a thickness of 0.4 mm, embedded in the brass mockup but isolated from the latter. The temperature fluctuation as a function of time was read at the initial instant of

the gust, while the wall temperature was still uniform. Since the mockup was solid, its temperature remained practically constant during the entire gust. After having made tests at various values of the ratio T_p/T_i, a practically linear curve can be plotted, representing q/T_i as a function of T_p/T_i. The slope of the tangent to this curve, for $T_i = T_p$, represents the density coefficient of the convective heat flux: $h = q/(T_p - T_r)$. The ratio T_r/T_i can be determined along this tangent, for $q = 0$. The angles of sweepback selected were 60°, 65°, 70°, 75°, 80°, 85°, 90°.

At Mach 7, the tests were made in the hypersonic wind tunnel of the IMFM by R.Guillaume. The base temperature was about $600^\circ K$ and the wall temperature slightly below $300^\circ K$. The test Mach number was 7.03.

The principle of determining the heat transfer is the same as at a Mach number of 4. However, it is impossible to sufficiently vary the ratio T_p/T_i so as to obtain a satisfactory accuracy in determining T_r and h. The thickness of the pellets was 3 mm in this case, while the angles of sweepback were 65°, 70°, 75°, 80°.

2.1.2 Tests at Mach Number 10 /891

The model B with a sweepback of 75° consisted of a spherical tip and a leading edge with a radius of 8 mm, at an overall length of 107 mm.

This model was tested in the hypersonic R 3 wind tunnel of the ONERA (National Aerospace Research and Development Administration) at Chalais-Meudon, at a test Mach number of $M_\infty = 9.85$. The base temperature and the wall temperature had a mean value of $T_i = 1180^\circ K$ and $T_p = 290^\circ K$, respectively.

The measuring principle for the heat transfer consisted in recording the temperature rise of the wall itself, as a function of time, and in defining the

heat transfer from the derivative dT/dt. The model consisted of an iron skin of a thickness of 1 mm, whose temperature was measured by means of thermocouples. The temperature fluctuation was read at the initial instant of the gust; operation with a bypass ensured, from this initial instant, the necessary base temperature. Thus, the measured heat fluxes refer to a uniform wall temperature, equal to the ambient temperature.

2.2 Results

2.2.1 Pressure Distribution at the Wall

The experimental investigation of the pressure was made mainly along the cylindrical portion of the leading edge, while the pressures along the spherical portion were theoretically determined. We used a Newtonian pressure law, extended by a Meyer-Prandtl expansion.

The measured pressure distributions, along the stagnation line of the leading edge, are plotted in Fig.1.

At Mach numbers of 4 and 7, the length of the mockups was sufficient for having the pressure shift rearward toward a rather constant value, close to that obtained for an infinite sweptback cylinder.

The development of the pressure at Mach 4, from the distribution observed on the spherical portion, proceeds in a highly regular manner tending rapidly toward a uniform asymptotic value. This is not the same for a Mach number of 7 at which a much more irregular development can be observed at the attachment point, where the pressure passes through a minimum which tends to shift downstream with increasing sweepback.

This latter phenomenon is even more pronounced at Mach 10. The length of the mockup apparently was insufficient to reach the asymptotic value of the

pressure corresponding to the infinite cylinder.

2.2.2 Form of the Shock Wave and Entropy Layer

To extend the data obtained in pressure measurements, the experimental program included an optical study of the shape of the shock wave, for each individual case. A schlieren method was used for accurately determining the trace of the shock wave in the plane of symmetry. A highly sensitive strioscopic visualization was used for obtaining data on the volume flow rate between the leading edge and the shock wave.

For illustration, the result is shown in Fig.2 where the development of /892 the shape of the shock with the sweepback angle is plotted at a Mach number of $M_\infty = 7$. Two modes of representation were used.

In the first version (upper diagram), the form of the shock wave relative to a fixed angle of attack is given. It is obvious that, at all sweepbacks, the trace of the shock wave, after first coinciding with that of a sphere, starts approaching the leading edge; this approach is closer the more the sweepback diminishes. A minimum of separation is observed at a sweepback of 65°. It seems that this distance then tends toward a constant value, at infinity downstream. The fluctuations in the pressure distribution at the attachment point are due to a reflection of the expansion waves, emerging from the wall after the sonic point, on the shock wave, on the stream surfaces (highly rotational flow), and on the sonic line. In other words, these fluctuations are a consequence of the nonviscous effects due to the blunting of the nose.

In the second version, the various shock waves are represented at a leading edge which is no longer fixed but set to the corresponding sweepbacks. This configuration permits observing the invariance of the shock wave of the sphere

and also shows the shift of the incipient influence of a cylindrical leading edge.

At Mach 7 and 10, the strioscopic visualization gives patterns as shown in Figs.3 and 4 and yields complementary data by indicating that a specific development of the volume flow rate takes place between wall and shock wave. Two different domains were observed, for the region between shock wave and obstacle. A low-density region, shown in black, was observed near the attachment point, developing with increasing angle of sweep. Apparently, this region characterizes a high-entropy zone, corresponding to the streamlines that have traversed the shock wave near its crest. The other region, shown in white, corresponds to the streamlines having traversed the shock wave in its oblique portion.

An attempt was made to define the phenomenon by measuring the Pitot pressures between the wall and the shock wave, at a Mach number of 7. Two examples of the obtained results in three abscissas are plotted in Fig.4, relative to the corresponding strioscopic visualizations. Since the static pressures are not known, an interpretation of the resultant curves becomes difficult. Near the point of transfer to the spherical tip, a considerable rise in Pitot pressure, at the interface between the boundary layer and the shock wave, apparently indicates the passage through a region of intense entropy gradient. Conversely, far from the tip, a much slower variation seems to indicate an isentropic flow whose stagnation pressure tends toward the pressure prevailing downstream of the oblique shock wave of the leading edge.

Apparently, a three-dimensional effect is involved here; the streamlines, after passing through the shock wave near its crest, first follow the leading edge and then drift away from this edge, traveling toward the plane faces of the wing. This effect is greater at less pronounced sweepback.

2.2.3 Distribution of the Heat Flux on the Wall

The results relative to the heat transfer, measured along the stagnation line of the leading edge, are plotted in Figs.4, 5, 6. In all cases, the experimental data are related to the calculated value at the stagnation point, by the Fay and Riddell formula.

At Mach 4, a relatively constant heat transfer along the cylinder is /893 obtained, with a value that decreases with increasing angle of sweepback.

This is not the same at Mach 7, as already demonstrated elsewhere (Bibl.3), and at Mach 10. The heat flux along the wall then undergoes a more irregular development in the region of transfer from sphere to cylinder. This development apparently, like that of the pressure, is directly related to the above-mentioned reflections, with the heat transfer passing through a minimum at an abscissa that corresponds distinctly to that of the pressure minimum.

3. Theoretical Study of Laminar Heat Transfer in Three-Dimensional Flow

3.1 Principle of Superposition and Form of the General Equations

Various authors (Bibl.4, 5) showed that a considerable simplification could be obtained in the three-dimensional boundary layer problem if the velocity component in the boundary layer, transverse to the exterior streamlines, could be assumed as low with respect to its longitudinal component. This principle of superposition of the longitudinal flow, which apparently is specifically applicable to wings with strong sweepback, permits treatment of the equations for longitudinal flow without having to allow for the equations of transverse flow. Using, as longitudinal axis, the projection of the exterior streamline onto the surface, and assuming that the transverse component v as well as its derivatives are low, the following system of local equations will be ob-

tained:

$$\rho u \frac{\partial u}{\partial s} + \rho w \frac{\partial u}{\partial y} = -\frac{\partial p}{\partial s} + \frac{\partial}{\partial y}\left(\mu \frac{\partial u}{\partial y}\right), \quad \text{equation of longitudinal motion} \qquad (1a)$$

$$\rho u \frac{\partial T_i}{\partial s} + \rho w \frac{\partial T_i}{\partial y} = \frac{\partial}{\partial y}\left[\mu\left(\frac{\partial T_i}{\partial y} + \frac{1 - P_r}{P_r}\frac{\partial T}{\partial y}\right)\right], \quad \text{equation of energy} \qquad (1b)$$

$$\frac{\partial}{\partial s}(\rho u e) + \frac{\partial}{\partial y}(\rho w e) = 0, \quad \text{equation of continuity} \qquad (1c)$$

where s denotes the measurements along the streamlines, while e represents a quantity proportional to the distance between two adjacent streamlines.

The total equations, obtained by integrating the local equations of motion and energy in accordance with the thickness of the boundary layer, will then read

/894

$$\frac{C_f}{2} = \frac{d\delta_2}{ds} + \delta_2\left[\frac{H + 2}{u_e}\frac{du_e}{ds} + \frac{1}{\rho_e}\frac{d\rho_e}{ds} + \frac{1}{e}\frac{de}{ds}\right], \quad \text{total equation of momentum} \qquad (2a)$$

$$\frac{q}{\rho_e u_e c_p T_{ie}} = \frac{d\Delta}{ds} + \Delta\left[\frac{1}{u_e}\frac{du_e}{ds} + \frac{1}{\rho_e}\frac{d\rho_e}{ds} + \frac{1}{e}\frac{de}{ds}\right], \quad \text{total equation of energy} \qquad (2b)$$

It becomes immediately obvious that the principle of superposition makes it possible to give the equations of the three-dimensional boundary layer a form identical to that of the boundary layer on a body of revolution whose ordinate of the meridian is assumed to be e(s). If the exterior flow of the perfect fluid is known, the reduced width e of the stream surface will, in principle, be a datum of the problem. In that case, any theoretical treatment, established for a flow of the form of a surface of revolution, can be used for calculating the

development of the three-dimensional boundary layer.

3.2 Methods of Calculation for the Heat Transfer to the Wall

3.2.1 Determination of the Streamline Divergence

Based on the principle of superposition, it is suggested to make use of calculation methods that incorporate local equations and the total equation of energy, with the practical purpose of predicting the heat flux at the wall of strongly sweptback wings and, specifically, along their leading edge.

For either one of the methods, it is necessary to determine the term (1/e) (de/ds) representing the divergence of the streamlines.

For an arbitrary surface, considerations of differential geometry permit demonstrating that e(s) is a solution of the differential equation

$$\frac{d^2e}{ds^2} + \left(K + k_2 - \frac{\partial k_2}{\partial n} \right) e = 0 \tag{3}$$

where K denotes the total curvature of the surface, while k_2 is the geodesic curvature of the streamline at the point under study. This latter can be estimated if the distribution of the flow quantities at the edge of the boundary layer is known:

$$k_2 = -\frac{1}{\rho_e u_e^2} \frac{\partial p}{\partial n} . \tag{4}$$

Posing $(1/e)de/ds = \phi(s)$, we obtain

$$\frac{d\phi}{ds} + \phi^2 = \frac{\partial k_2}{\partial n} - k_2^2 - K \tag{5}$$

Equation (5) is of the first order in ϕ. The second term, in general, /895 is analytically not known. A stepwise construction of the streamlines, however, would permit a numerical integration. This will yield

$$\frac{e(s)}{e(s_1)} = \exp\left(\int_{s_1}^{s} \phi(s)\,ds\right)$$

where s_1 is the abscissa of a point for which $\phi(s)$ is arbitrarily fixed. [The function e(s) is determined to within a multiplicative constant.]

In the case of interest here, the total curvature K is zero along the cylindrical portion. The abscissa s_1 will be taken as equal to that corresponding to the attachment point with the spherical tip. The stagnation line will be assumed as the nonsingular streamline ($k_2 = 0$).

Then, eq.(5) becomes

$$\frac{d\phi}{ds} + \phi^2 = \frac{\partial k_2}{\partial n}. \tag{6}$$

Along the spherical sector, the value for e can be taken as $e = \sin \frac{s}{R}$.

The initial value of ϕ at the shoulder will thus be: $\phi(s_1) = \frac{\cot \Lambda}{R}$. In general, the derivative $\partial k_2/\partial n$ is not known analytically along the line of separation. If $\partial k_2/\partial n$ is identically zero, the streamlines close to the separation line may be compared to geodesic lines issuing from the stagnation point. This case can take place only in the vicinity of $\Lambda = 90^\circ$ and has been studied elsewhere (Bibl.6).

For an infinite cylinder, the following relations can be established along the stagnation line:

$$\frac{R}{e}\frac{de}{ds} = \frac{R}{u_e}\frac{dv}{dn} \tag{7}$$

$$\frac{\partial k_2}{\partial n} = \left(\frac{R}{u_e}\frac{dv}{dn}\right)^2. \tag{8}$$

These relations are located at infinity in the case investigated here. However, at a finite distance, the origin effect, created by the attachment

point with the spherical tip, must be taken into consideration, specifically in the presence of a pressure generation. The study proposed elsewhere (Bibl.2), making use of eq.(7) at a finite distance, is thus only asymptotically valid.

3.2.2 Method of Local Similitude /896

As mentioned at the beginning of this Chapter, any theoretical treatment established for a flow of revolution can be used if the principle of superposition is assumed and if the function e(s) is known. In this manner, the calculation of transfer was presented by Valensi (Bibl.6) for the case in which the streamlines, at the edge of the boundary layer projected onto the surface, coincide with the geodesic lines issuing from the impact point. The calculation was performed by extension of the Stine and Wanlass method (Bibl.7), applicable to axisymmetric flows. The method is here extended to the case where e(s) is defined by eq.(6).

The calculation suggested by Stine and Wanlass makes successive use of the Mangler and Stewartson transformations and reduces the problem to that of an incompressible two-dimensional flow. It then becomes possible to use the similar solutions of the laminar boundary layer, based on the Falkner-Skan model. The fundamental parameter, permitting a local correspondence, is $m = (s/u_e)\, du_e/ds$, which becomes $\bar{m}$ and $\bar{\bar{m}}$ in each of the associated two-dimensional flows.

Thus, it is assumed that, at each point, an incompressible two-dimensional flow can be made to correspond to the real flow, with the velocity being distributed in accordance with a law in powers of the abscissa, having an exponent of $\bar{\bar{m}}$.

Thus, for the local coefficient of the flux density of the convective heat transfer to the wall, we have

$$h = k_e \left[\frac{u_e}{\nu_e s} \frac{m}{\bar{m}} \frac{\bar{\bar{m}}}{\bar{\bar{m}}} \left(1 + \frac{\gamma - 1}{2} M_e^2\right) \left(\frac{\bar{\bar{m}} + 1}{2}\right) \right]^{1/2} \left(\frac{d\theta}{d\eta}\right)_{\substack{\eta=0 \\ \bar{\bar{m}}}} \qquad (9)$$

where $(d\theta/d\eta)_{\substack{\eta=0 \\ \bar{\bar{m}}}}$ is the temperature gradient at the wall for the corresponding incompressible two-dimensional flow.

The parameters $\bar{m}/m$ and $\bar{\bar{m}}/\bar{m}$ are given by $\frac{\bar{m}}{m} = \frac{\int_0^s e^2 ds}{e^2 s}$

$$\frac{\bar{\bar{m}}}{\bar{m}} = -\left(1 + \frac{\gamma - 1}{2} M_e^2\right)^{\frac{5\gamma - 3}{2\gamma - 1}} \frac{1}{\bar{s}} \int_0^{\bar{s}} \left(1 + \frac{\gamma - 1}{2} M_e^2\right)^{-\frac{3\gamma - 1}{2(\gamma - 1)}} d\bar{s} .$$

The reduced temperature gradient $(d\theta/d\eta)_{\substack{\eta=0 \\ \bar{\bar{m}}}}$ is tabulated for various ratios T_p/T_i and for temperature distributions at the wall that can be proportional to a power of $\bar{\bar{s}}$.

The heat transfer q can then be calculated, provided that the recovery /897 factor r is known. This value is taken as equal to $p_r^{1/2}$, for $P_r = 0.7$.

3.2.3 Method Based on the Total Equation of Energy

It has been demonstrated (Bibl.8) that a flexible calculation method, based on a solution of the total equation of momentum, would permit predicting - with a reasonable approximation - the principal dynamic characteristics of a laminar or turbulent boundary layer, in the case of moderate pressure gradients. The approximate method used here for calculating the heat transfer is an extrapolation of this technique to the total equation of energy.

The basic hypothesis, used for the dynamic problem, is to assume that the shape of the velocity and temperature profiles in the boundary layer varies only little, so that the friction coefficient, as a function of the Reynolds number of the thickness of the momentum, can be expressed by the relation of

the plane plate. Using the concept of reference temperature, the relation applicable for the friction coefficient then becomes

$$\frac{C_f}{2} = \frac{0.2205q}{\left(\frac{\rho_e u_e \delta_2}{\mu_e}\right)} g \quad \text{with} \quad g = \frac{\rho^* \mu^*}{\rho_e \mu_e} \tag{10}$$

where g is the C_f/C_{f1} of the laminar plane plate at constant R_{δ_2}. This value is obtained from the volume mass ρ^* and from the viscosity μ^*, which correspond to the reference temperature T^*. For the latter, we suggest the use of Monaghan's relation

$$T^* - T_e = 0.54(T_p - T_e) + 0.16(T_f - T_e) \tag{11}$$

where T_f is the temperature of the athermal wall, to which a recovery factor of $r = P_r^{1/2}$ is assumed to correspond.

The same treatment will now be applied to the total equation of energy, considered as a differential equation for the energy thickness Δ. For integrating this equation, we use the relation expressing the heat flux at the wall as a function of the Reynolds number of the energy thickness, based on the properties of the plate.

For a laminar plane plate, at constant wall temperature, a constant ratio of the heat flux coefficient to the friction coefficient exists:

$$S = C_h \Big/ \frac{C_f}{2} \doteq P_r^{-2/3} .$$

From eq.(10), which expresses C_f as a function of R_{δ_2}, it is easy to derive - after integration of the total equations of the plane plate - the relation that expresses the heat flux at the wall as a function of the Reynolds number of the energy thickness:

$$\frac{q}{\rho_e u_e c_p T_{i_e}} = \frac{B}{\left(\frac{\rho_e u_e \Delta}{\mu_e}\right)} \quad \text{with} \quad B = 0.2205 g \left(S \frac{T_p - T_f}{T_{i_e}}\right)^2 \qquad (12)$$

/898

a relation that transforms the total equation of energy (2b) into a linear differential equation of the first order for Δ^2.

In the general case, the integration is made from the point s_0 where the energy thickness is known. This yields the energy thickness of

$$(\Delta \rho_e u_e e)^2 = (\Delta \rho_e u_e e)^2_{s_0} + \int_{s_0}^{s} 2B \rho_e \mu_e u_e e^2 ds \quad . \qquad (13)$$

The heat flux at the wall can be obtained from this, by using eq.(12).

In the problems of interest here, the starting point of the integration will be the stagnation point of the body front. The ratio of the heat flux at the moving point to that at the stagnation point can be conveniently expressed by the formula

$$\frac{q}{q_i} = \frac{\frac{B}{B_i} \frac{\rho_e \mu_e}{\rho_i \mu_i} u_e e}{2 \left[\left(\frac{du_e}{ds}\right)_i \int_0^s \frac{B}{B_i} \frac{\rho_e \mu_e}{\rho_i \mu_i} u_e e^2 \, ds \right]^{1/2}} .$$

3.3 Application to the Leading Edge and Comparison with Experiment

Two domains must be differentiated in application of the calculation to the cases in question.

A first region is formed by the spherical sector, forming the tip for which the flow and the heat transfer are those of a forward body of revolution. The reduced width of the stream surface is here simply proportional to the distance of the wall from the axis that carries the stagnation point and the center of the sphere.

A second region, which has its origin at the attachment point with the cylinder is the leading edge itself. Here, the problem is that of a three-dimensional flow containing pressure gradients determined by experiment. In view of the observations made previously on the origin effect, no other possibility exists at present than to use, in the calculation, a stagnation pressure at the edge of the boundary layer equal to the stagnation pressure p_1' downstream of the straight shock shed from the nose. In all these cases, the experimental pressure curves will be used for calculating the heat flux.

Data obtained by Michel (Bibl.2) were used for obtaining the divergence of the streamlines, where an approximate relation expresses this divergence as a function of the normal velocity gradient and assumes a Newtonian transverse pressure distribution:

$$\frac{R}{e}\frac{de}{ds} = \frac{R}{u_e}\frac{dv}{dn} = \frac{1}{M_e}\left[\frac{2}{\gamma}\left(1 - \frac{p_\infty}{p_e}\right)\right]^{1/2} .$$

The geometrical study given in Section 3.2.1 demonstrates that this re- /899
lation is only rigorous in the case of a purely cylindrical flow, i.e., at a great distance from the nose.

In the region of varying pressure close to the attachment point, a determination of the streamline divergence must include an integration of eq.(6). This integration is made by using the following approximate value for $\partial k_2/\partial n$:

$$\frac{\partial k_2}{\partial n} = \left(\frac{R}{u_e}\frac{dv}{dn}\right)^2$$

which is rigorously valid for a purely cylindrical flow.

On the other hand, dv/dn was calculated by assuming a Newtonian transverse distribution, from the pressure measured along the stagnation line.

The initial value, taken at the shoulder and imposed by the preceding flow of revolution, as demonstrated in Section 3.2.1, can be expressed by

$$\left[\frac{R}{e}\frac{de}{ds}\right]_{s=s_1} = \cot \Lambda .$$

At Mach 4, the constancy of the pressure and of the heat transfer, over most of the length of the leading edge, have resulted in applying only an asymptotic form of the integral method, a form referring to a cylindrical flow of uniform pressure with a stagnation pressure of p_t'. The broken curves, plotted to the right of the experimental curves in Fig.5, agree satisfactorily with the measured values.

At Mach 7, the calculations included an application of local and general methods in the pressure gradient of the leading edge. The corresponding curves, plotted in Fig.5, demonstrate that each of these two methods satisfactorily reproduces the experimentally observed development, in that the flux, in the region influenced by the attachment point, passes through a minimum. However, it should be noted that the similitude method enters the exterior velocity gradient as well as the divergence of the streamlines in a direct and local manner. The application of this method becomes difficult for wings of medium sweepback, in the region influenced by the attachment point, because of the inaccuracy in the Mach number distribution, determined from the pressure at the wall.

Figure 6 shows the results obtained with the integral method at a Mach number of 10. This method still stipulates a minimum heat flux, corresponding largely to that of the pressure. A more rigorous determination of the width of the stream surface apparently will lead to results that are in better agreement with experimental data than those obtained elsewhere (Bibl.2).

At strong sweepback, experiment and calculation agree over the entire

length of the model. At sweep angles of 50° and 60°, experiments are first in satisfactory agreement with the calculation but then yield a heat flux value that steadily decreases to below the calculated values. In fact, the trend /900 is toward a new asymptotic value, which can be determined by applying the integral method to a uniform cylindrical flow whose stagnation pressure would have a value of p_{t_2} relative to the downstream section of an oblique shock parallel to the leading edge. This result can be compared to the observations made on the influence of entropy gradients produced by the curvature of the shock wave.

4. Conclusions

An experimental and theoretical study, at Mach numbers of 4, 7, and 10 on the flow and heat transfer along the leading edge of hypersonic wings at various angles of sweepback led to the following conclusions:

An appreciable increase in Mach number and pressure occurs at high velocity along the leading edge of a real wing, within a region influenced by the attachment point between the forward body and the actual leading edge. This increase involves noticeable variations of the heat transfer to the wall.

For predicting the heat transfer to the wall, it is necessary to allow for the influence of the pressure gradients in the development of the three-dimensional boundary layer. An application of the principle of superposition permits establishing calculation methods that, at strong sweepback, will yield results in satisfactory agreement with experiments.

Tests made at high Mach number and medium sweep indicate an influence of the entropy gradients, due to the curvature of the shock wave, which must lead to a variation in the stagnation pressure at the edge of the boundary layer.

BIBLIOGRAPHY /901

1. Reshotko, E. and Beckwith, I.E.: Compressible Laminar Boundary Layer over a Yawed Infinite Cylinder with Heat Transfer and Arbitrary Prandtl Number. NACA TN 3986, June 1957.

2. Michel, R. and Duong, V.H.: Heat Flux at the Leading Edge of a Wing with Strong Sweepback (Flux de chaleur au bord d'attaque d'une aile en forte flèche). Congrès I.C.A.S., T.P. O.N.E.R.A., No.116, 1964.

3. Valensi, J. et al.: Influence of the Mach Number and the Angle of Sweepback on the Distribution of the Heat Flux Transferred by Convection along the Separating Line of the Hemicylindrical Leading Edge of a Delta Wing with a Spherical Sector Nose at Zero Angle of Attack (Influence du nombre de Mach et de l'angle de flèche sur la distribution du flux de chaleur convectée le long de la ligne de separation du bord d'attaque hemicylindrique d'une aile en delta à pointe en secteur sphérique et sous incidence nulle). Compt. Rend. Acad. Sci., No.259, p.2174, October 1964.

4. Eichelbrenner, E.A. and Oudart, A.: Calculation Method for the Three-Dimensional Boundary Layer (Méthode de calcul de la couche limite tridimensionnelle). Publication O.N.E.R.A., No.76, 1955.

5. Cooke, J.C. and Hall, M.G.: Boundary Layers in Three Dimensions. British RAE Rep.Aero 2635.

6. Valensi, J. and Guffroy, D.: A Calculation Method for the Local Convection Coefficient (Hypersonic Flows, Three-Dimensional Laminar Boundary Layer) [Sur une méthode de calcul du coefficient de convection local (écoulements hypersoniques, couche limite laminaire tridimensionnelle)]. Compt. Rend. Acad. Sci., No.259, p.2344, October 1964.

7. Stine, H.A. and Wanlass, K.: Theoretical and Experimental Investigation of

Aerodynamic Heating and Isothermal Heat Transfer Parameters on a Hemispherical Nose with Laminar Boundary Layer at Supersonic Mach Numbers. NACA TN 3344, December 1954.

8. Michel, R.: Turbulent Boundary Layers and Practical Calculation of Boundary Layers in Compressible Fluid (Couches limites turbulentes et calcul pratique des couches limites en fluide compressible). T.P. O.N.E.R.A., No.25, 1963.

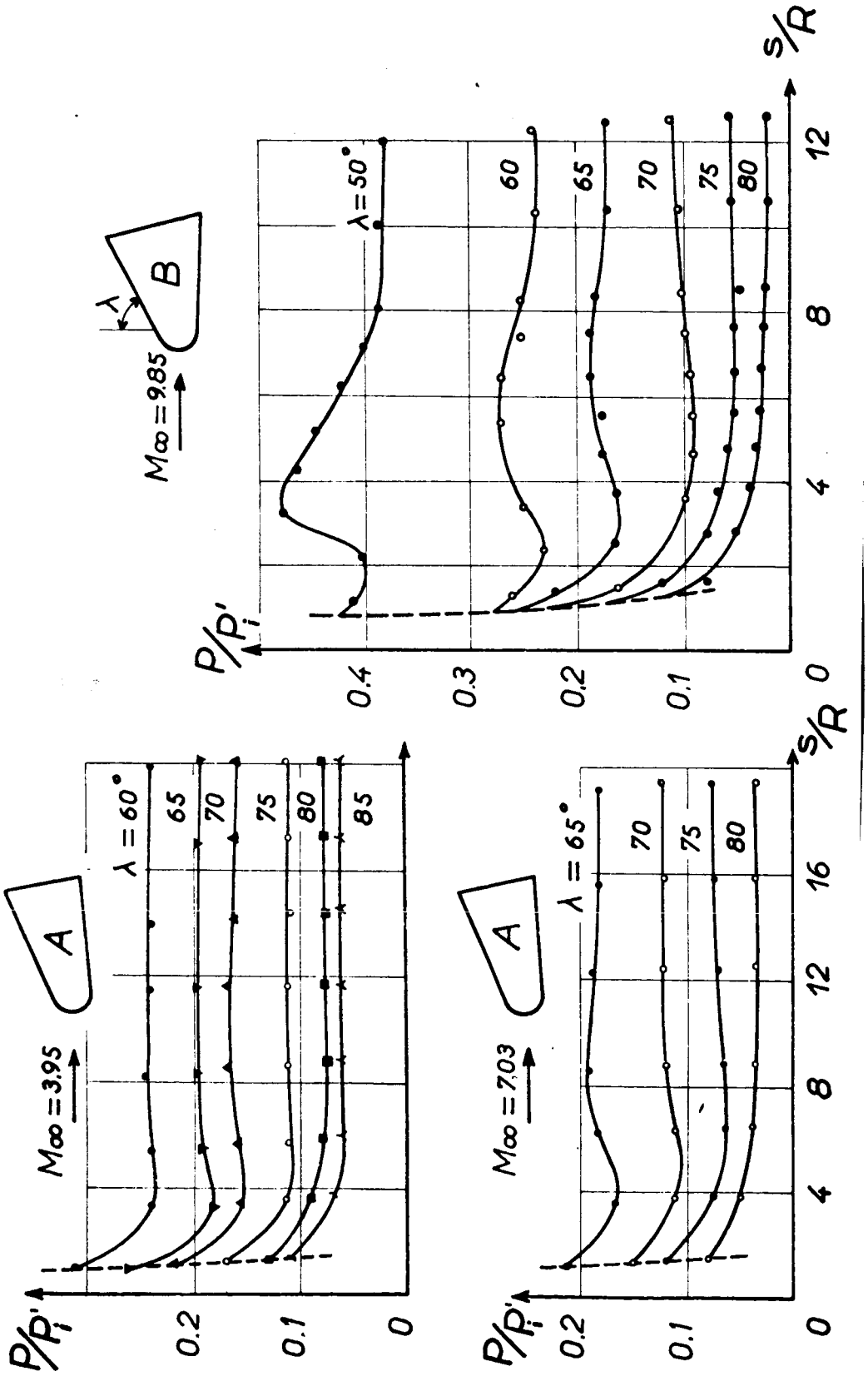

Fig.1 Pressures at the Leading Edge

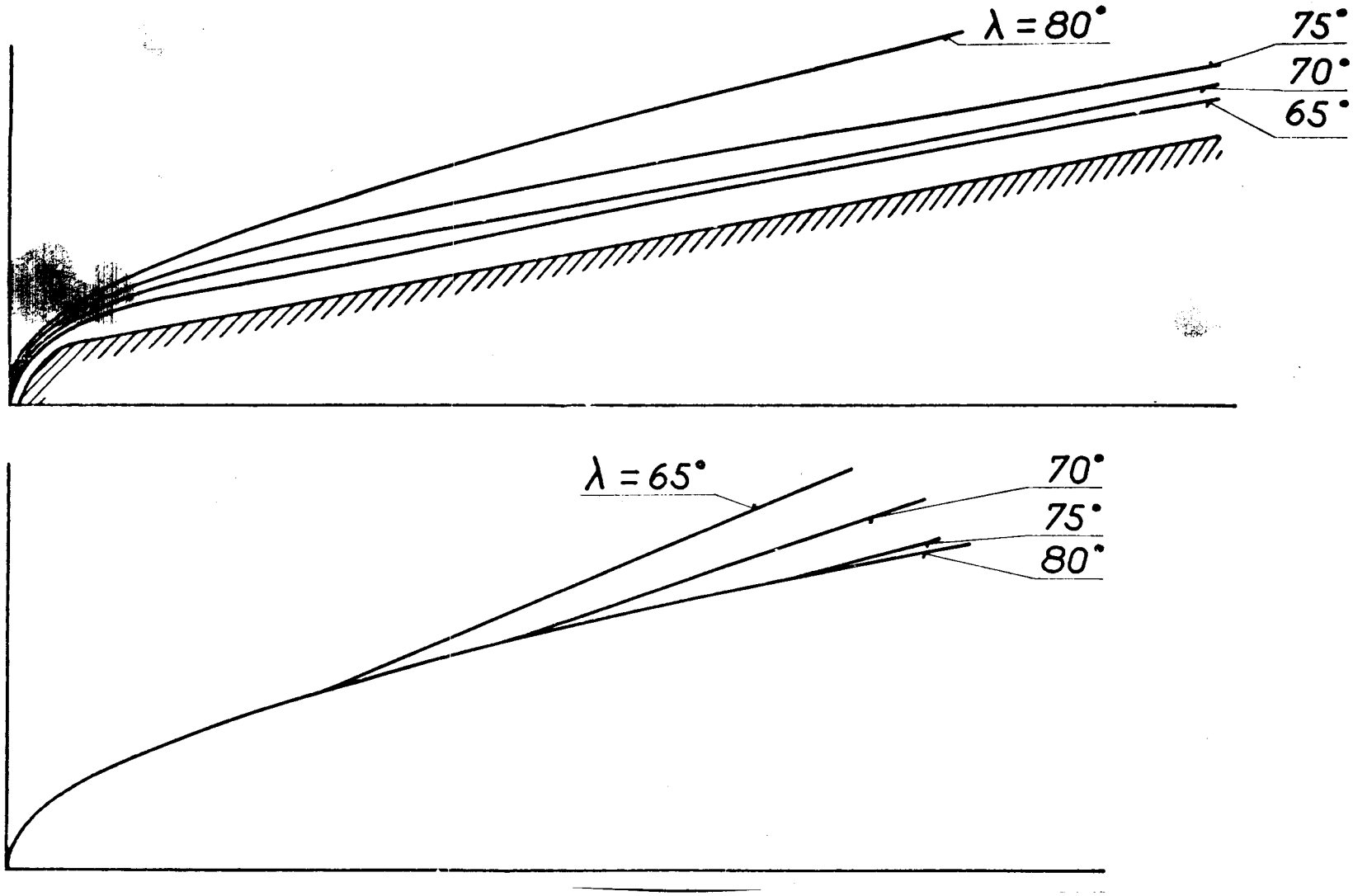

Fig.2 Shock Waves at Mach M_∞ = 7.03 (Model A)

/904

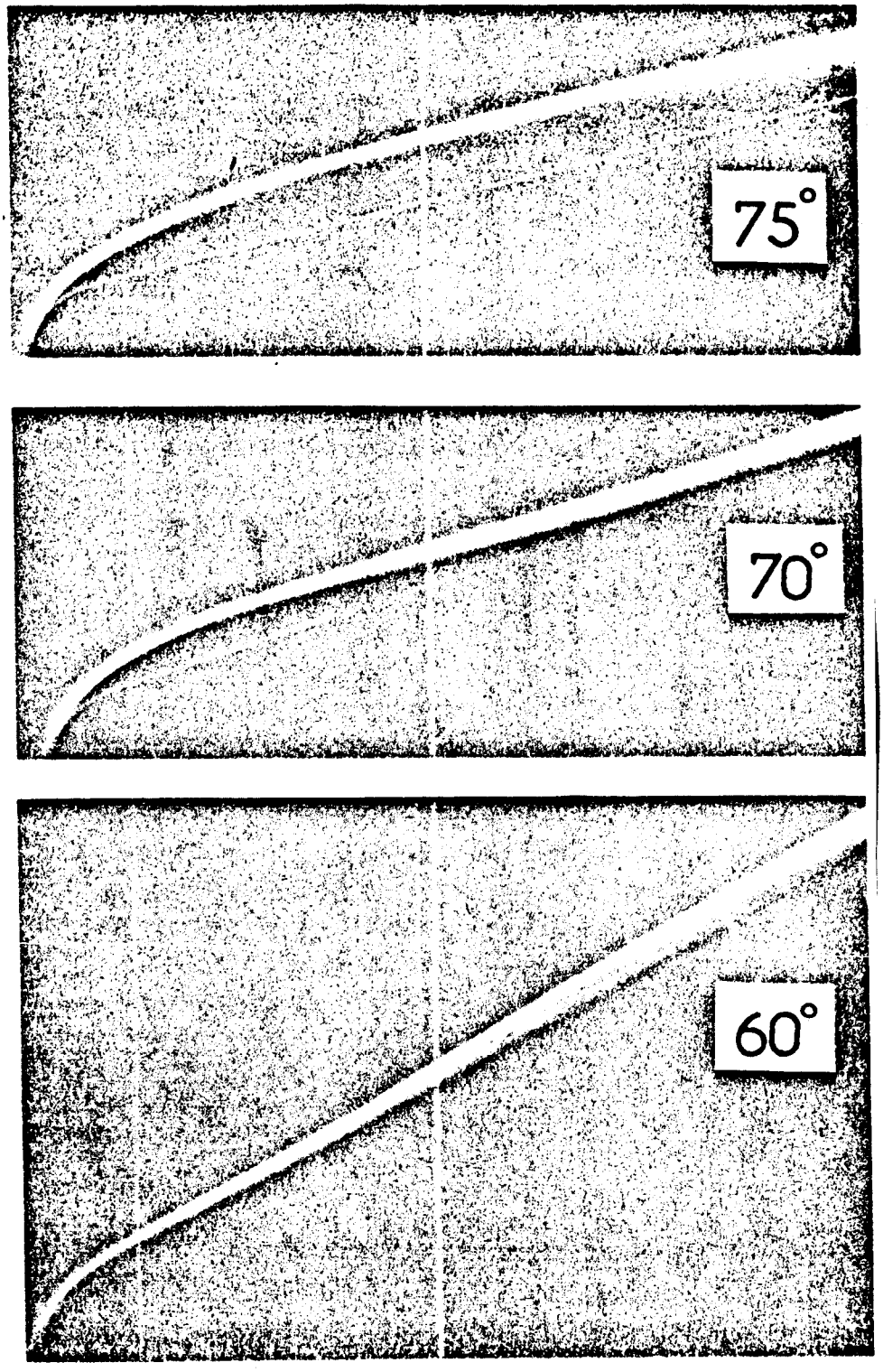

Fig.3 Shock Waves at M_∞ = 9.85 (Model B)

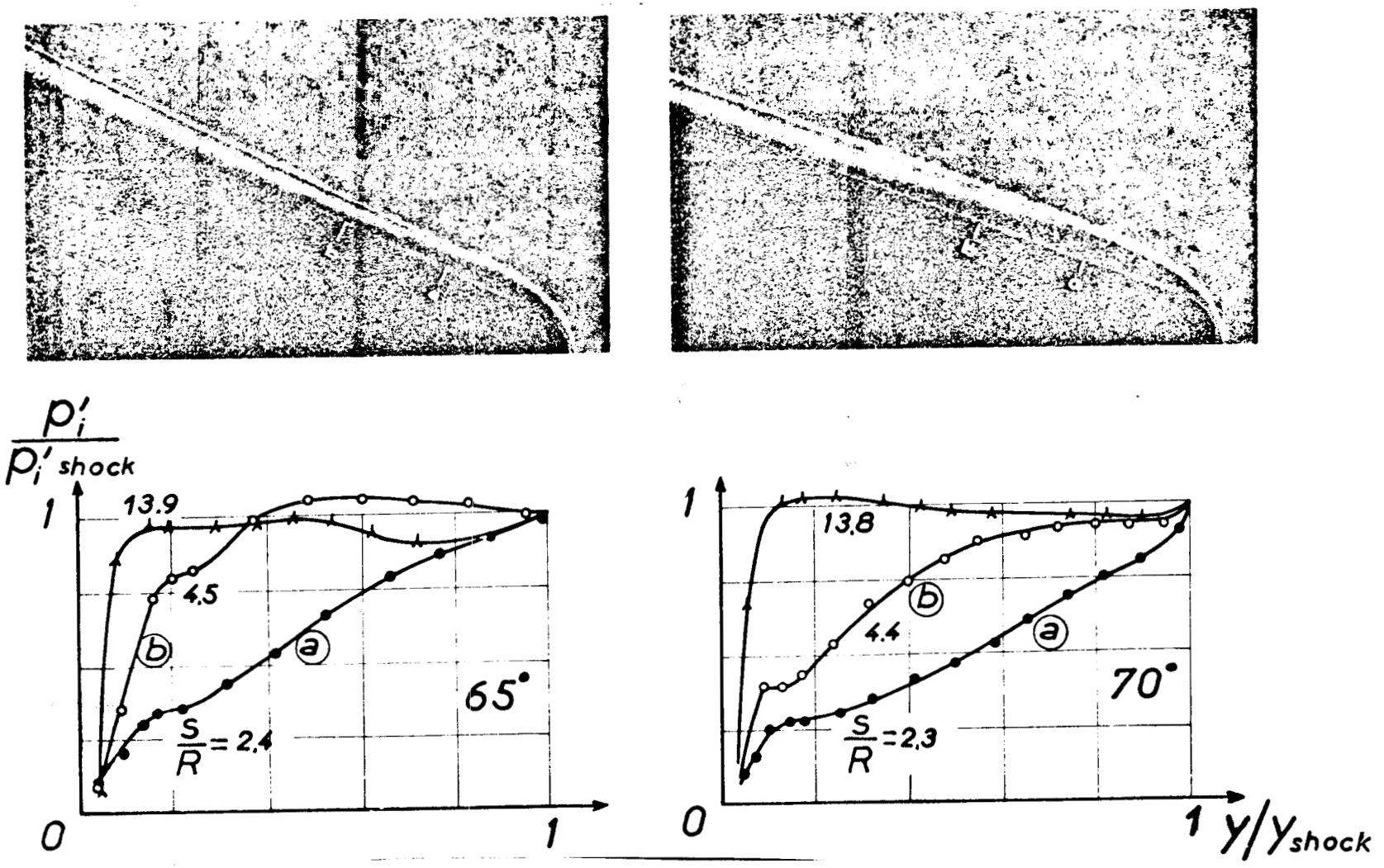

Fig.4 Shock Waves and Pitot Pressures (Model A, M_∞ = 7.03)

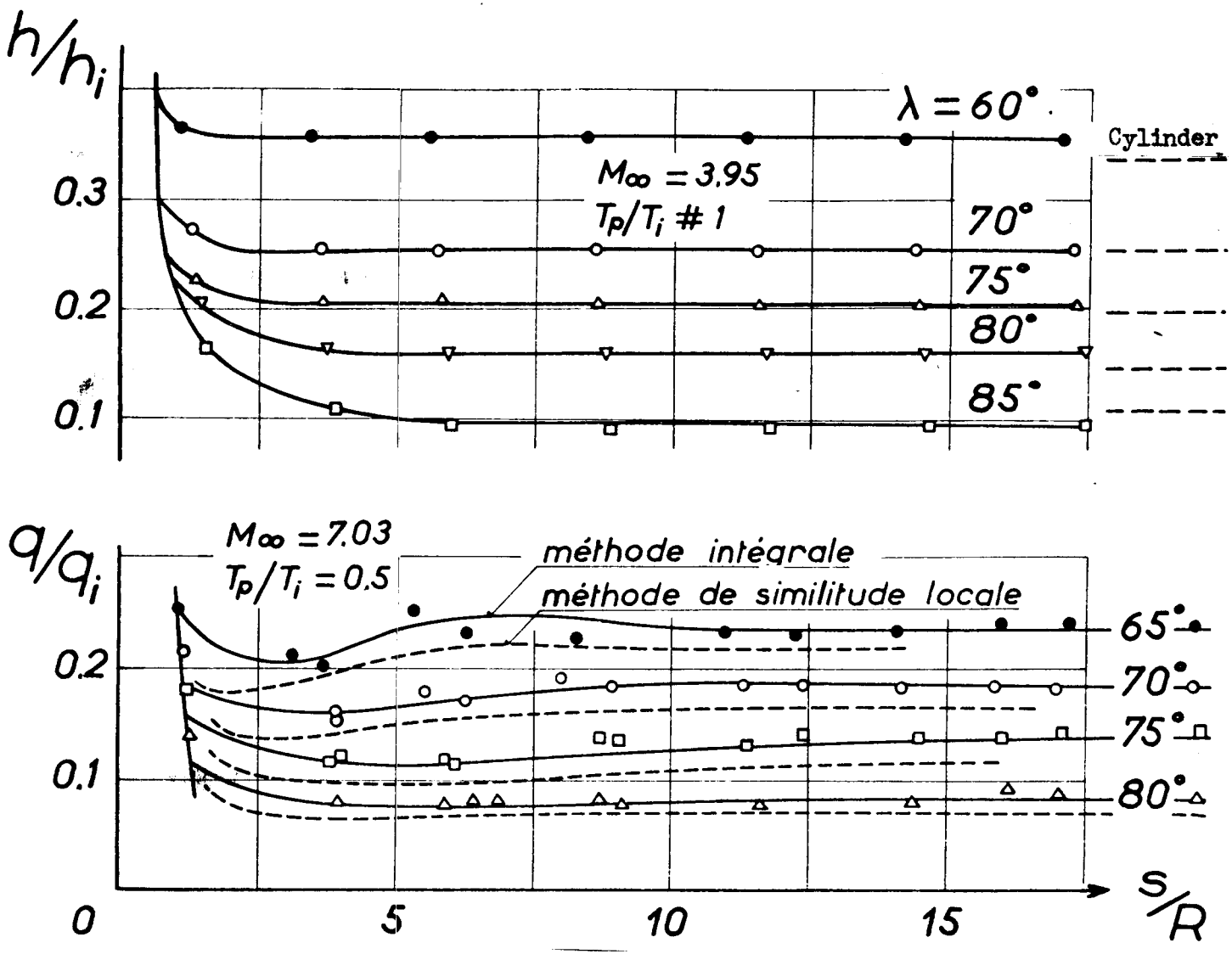

Fig.5 Heat Flux at the Leading Edge of the Model A

/907

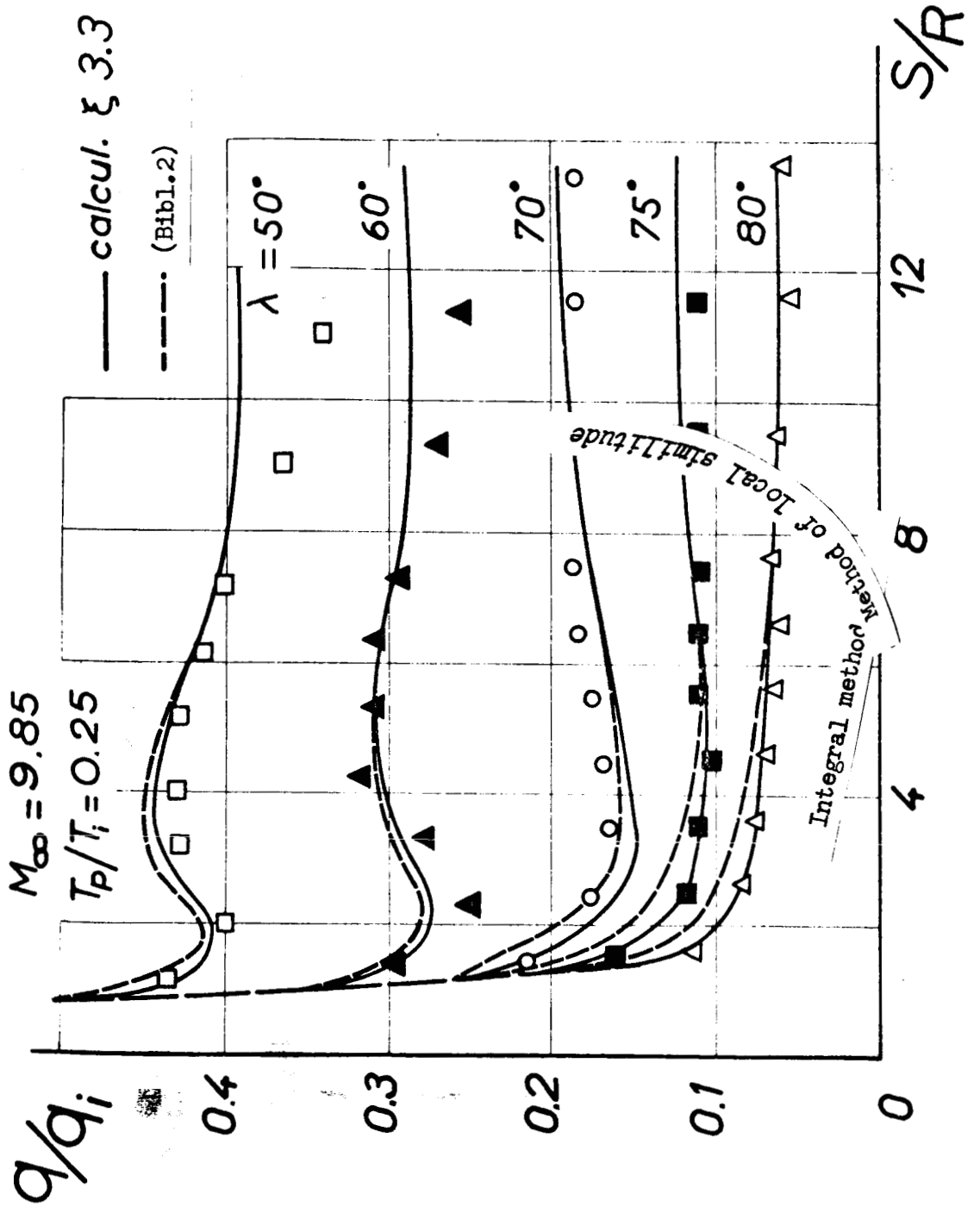

Fig.6 Heat Flux at the Leading Edge of the Model B